Ionics (2022) 28:4311–4319
https://doi.org/10.1007/s11581-022-04651-y

ORIGINAL PAPER

# Chemical diffusion and ionic conductivity in nonstoichiometric nanocrystalline superionic $Na_xCu_{1.75}S$ ($x = 0.1, 0.15, 0.2, 0.25$) materials

K. A. Kuterbekov[1] · M. Kh. Balapanov[2] · M. M. Kubenova[1] · R. Kh. Ishembetov[2] · M. Kh. Zeleev[3] · R. A. Yakshibaev[2] · A. M. Kabyshev[1] · R. A. Alina[1] · K. Zh. Bekmyrza[1] · B. U. Baikhozhaeva[1] · E. T. Abseitov[1] · L. U. Taimuratova[4]

Received: 9 March 2022 / Accepted: 17 June 2022 / Published online: 14 July 2022

**Abstract**

The paper presents the experimental results on ionic conductivity and chemical diffusion in nonstoichiometric nanocrystalline superionic materials $Na_xCu_{1.75}S$ ($x = 0.1$, 0.15, 0.2, 25). High values of the coefficient of conjugated chemical diffusion of cations and electronic holes ($1.1 \bullet 10^{-3}$ and $1.65 \bullet 10^{-3}$ cm$^2$/s at 410 °C) were observed in the studied electron-ionic conductors $Na_{0.10}Cu_{1.75}S$ and $Na_{0.20}Cu_{1.75}S$. Activation energies of the total ionic conductivity are measured as 0.30 and 0.40 eV for superionic $Na_{0.10}Cu_{1.75}S$ and $Na_{0.15}Cu_{1.75}S$ phases respectively. In the superionic phases, the measured values of the total ionic conductivity are 2.8, 1.5, and 2.0 S/cm for $Na_{0.10}Cu_{1.75}S$, $Na_{0.15}Cu_{1.75}S$, and $Na_{0.20}Cu_{1.75}S$ at 410 °C respectively. Thus, insertion of sodium to copper sulfide did not lead to worse of high ionic conductivity in the superionic phase.

**Keywords** Chemical diffusion · Ionic conductivity · Superionic materials · Copper chalcogenides · Synthesis

## Introduction

The main reason hindering the creation of competitive sodium-ion batteries (NIA) is the low efficiency of the available electrode materials. In addition, the sodium-ion electrochemical system has a serious drawback—a very long charge/discharge time—since NIAs cannot yet operate at high current densities due to the low diffusion rate [1, 2]. However, an intensive search for promising sodium storage electrode materials continues to develop. In recent works [3, 4], for example, methods have been proposed for the synthesis of hollow nanostructures for sodium storage. In paper [3], the as-prepared copper phosphide hollow nanocubes deliver a stable capacity of 325 mA•h·g$^{-1}$ at 50 mA·g$^{-1}$ and fast charging and discharging via pseudocapacitance behavior. The outstanding electrochemical performance by Zhe Hu et al. [3] is explained by the synergetic effects of high electronic conductivity of copper and the high sodium storage capability of phosphorus. In another work by L. Han et al. [4], hierarchically porous $MoS_2$-C hollow rhomboids (MCHRs) have been creatively synthesized via a facile self-templated solvothermal approach. It has been clarified that the obtained MCHRs assembled beneath ultrathin γ-MnS and carbon cohybridized $MoS_2$ nanosheets under the structural direction of the $MnMoO_4 \cdot 0.49 \bullet H_2O$ self-template. The prepared MCHR anode of sodium-ion batteries exhibited an excellent reversible capacity of 506 mA•h•g$^{-1}$ at 0.1 A•g$^{-1}$, ultrahigh rate capabilities up to 10 A•g$^{-1}$ with 310 mA•h•g$^{-1}$, and exceptional stability over 3000 cycles.

Copper chalcogenides have already shown themselves to be promising materials for NIA [5, 6]. These materials are good thermoelectrics too [7–9].

In this work, highly nonstoichiometric phases of copper sulfide (roxbyite and anilite) in the nanosized state are considered candidates for sodium storage materials, which can exhibit superionic properties at room temperature and, in addition, have a high electronic conductivity of $10^2$–$10^3$ Ohm$^{-1}$ cm$^{-1}$ [7–9]. The presence of a large number of copper vacancies in the structure of roxbyite (digenite) and anilite can dampen mechanical stresses in the lattice and increase the cyclability of the electrode material to 100 or more [5, 6].

---

✉ M. M. Kubenova
kubenova.m@yandex.kz

1 L.N.Gumilyov Eurasian National University, 2 Satpayev Str., Nur-Sultan, Kazakhstan

2 Bashkir State University, 32 Zaki Validi Str., Ufa, Russia

3 Bashkir State Medical University, 3 Lenina Str., Ufa, Russia

4 Caspian University of Technology and Engineering Named After Sh. Yessenov, Microdistrict 32, Aktau, Kazakhstan

When there is a gradient of the degree of nonstoichiometry in the sample, then there is also a gradient of the chemical potential of cations and anions, under the influence of which the diffusion of cations and anions towards each other occurs. The local electroneutrality of the sample is maintained by an equivalent electron flux. This process is usually called a chemical diffusion [10]. In the case of copper chalcogenides, anions can be considered practically immobile, and therefore, chemical diffusion means conjugated (ambipolar) diffusion of cations and electrons in a chemical field due to the gradient of the degree of nonstoichiometry and in an electric field arising due to the difference in the mobility of particles of different types.

Thus, chemical diffusion is associated with the self-diffusion of cations, the mobility of electron carriers, nonstoichiometry parameters, and through them—with the defective structure of the crystal. The study of chemical diffusion is important in practical terms, since it plays an important and often decisive role in many natural and technological processes determined by solid-phase chemical reactions: oxidation of metals, solid-phase synthesis of materials, transfer processes in energy devices with superionic materials. The process of conjugated chemical diffusion of ions in copper chalcogenides proceeds under the influence of a gradient of the degree of nonstoichiometry [10]. The conjugate chemical diffusion coefficient (CCDC) determines the rate at which chemical equilibrium is established. Since the condition of the electroneutrality of the sample in each cross section of the sample must be satisfied due to the compensation of charge transfer of ions by the transfer of electrons (holes), diffusion jumps of ions lead to the same displacement of matter as jumps of neutral atoms.

The internal electric field arising in the sample accelerates the movement of "slow" particles (cations) and accelerates the movement of "fast" particles (electrons). This explains the high values of the CCDC observed in comparison with the self-diffusion coefficients of cations.

According to VN Chebotin [10], the coefficients of the conjugated chemical diffusion of ions and electrons in solids can be expressed as

$$\tilde{\mathbf{D}} = t_i \tilde{\mathbf{D}}_{\mathbf{e}} + t_e \tilde{\mathbf{D}}_{\mathbf{i}} \qquad (1)$$

where $t_i = \sigma_i/(\sigma_e + \sigma_i)$ and $t_e = \sigma_e/(\sigma_e + \sigma_i)$ are ion and electron transport numbers and $\tilde{D}_i$ and $D_e$ are the individual chemical diffusion coefficients for ions and electrons (electron holes) respectively.

Sh. Miyatani showed in [11] that the time dependence of the potential difference $U_{ii}$ between two Ag|AgJ ion probes after switching off the stationary current through the Ag/AgJ/$Cu_xAg_{2-x}Se$/AgJ/Ag cell, as in the case of one type of mobile cations, described by the expression:

$$U_{ii}(t) = \frac{8}{\pi^2} \frac{jL}{\sigma_i} t_e \exp\left(-\frac{\pi^2 \tilde{D}_t}{L^2}\right) \qquad (2)$$

where $j$ is the current density at the moment of switching off, $\sigma_i = \sigma_{Ag+} + \sigma_{Cu+}$ is the total ionic conductivity, $L$ is the length of the sample, $t_e$ is the electronic transport number, and $\tilde{D}$ is the coefficient of the conjugate chemical diffusion of cations and electrons.

We believe that Miyatani's conclusions can be extended to other materials with high electronic conductivity and with two types of mobile cations, and, in particular, to the $Na_xCu_{1.75}S$ system, in which the $Na^+$ and $Cu^+$ ions are mobile. So, the chemical diffusion coefficient of $Na_xCu_{2-y}S$ superionic materials in this work was determined from the time dependence of the concentration polarization decay after switching off the current through the Cu/CuBr/Sample/CuBr/Cu electrochemical cell with reversible Cu/CuBr ion electrodes using Eq. (2).

This work is an attempt to study chemical diffusion and ionic conductivity in the $Na_xCu_{1.75}S$ system in order to elucidate the effect of sodium content on ion transport conditions. The first measurements of the conjugated chemical diffusion coefficient in the copper sulfide phases of chalcocite and djurleite at room temperature were made in 1983 by H. Rickert, H.D. Wiemhofer, and U. Tinter using the point electrode method [12–14]. H. Rickert and H.D. Wiemhofer revealed a CCDC maximum of $1.0 \bullet 10^{-6}$ $cm^2/s$ for chalcocite close to stoichiometric composition ($Cu_{1.999}S$), and a decreasing in CCDC with a nonstoichiometricity increasing. U. Tinter and H.D. Wiemhofer found a similar dependence of CCDC on nonstoichiometricity for djurleite ($2.4 \bullet 10^{-8}$ $cm^2/s$ for the $Cu_{1.957}S$ composition and then a decrease in CCDC with a nonstoichiometricity increasing). An analysis of all known results on CCDC at room temperature is presented by S. Cassaignon et al. in 1998 [15]. Also the work of Balapanov M.Kh. is known on studying of the dependence of ionic conductivity and CCDC in copper selenide on the size of crystallite grains at different temperatures [16]. CCDC in copper chalcogenides doped with silver and lithium were studied in [11, 17–21]. Ionic conductivity in sodium-doped copper sulfide $Na_{0.2}Cu_{1.8}S$ was recently reported in the study [9], in which it was noted that doping with sodium did not significantly affect the ionic conductivity of copper sulfide: the ionic conductivity increases exponentially up 1.5 to 2.3 S $cm^{-1}$ in the temperature range up 630 to 690 K. Observed values are comparable with the level of the ionic conductivity of the binary copper sulfide. In this paper, we present the results of measurements of the conjugate chemical diffusion coefficient in nonstoichiometric nanocrystalline superionic $Na_xCu_{1.75}S$ ($x = 0.1$, 0.15, 0.2, 0.25) materials in the same temperature range.

## Experimental methods

The synthesis reaction is carried out in a melt of NaOH and KOH hydroxides. It is known that the melting point of pure NaOH is 323° C, and for KOH, the melting point is 404° C. With a quantitative ratio between NaOH/KOH = 51.5:48.5, the melting point of the mixture decreases to 165 °C.

First, the prepared mixture of sodium and potassium hydroxides in the ratio is put into a Teflon vessel and heated to melting (about 165° C). Heat is supplied to the vessel both from the bottom and along the side walls for uniform heating throughout the volume. The lid of the vessel should not be tight so that excess vapors can freely escape from the vessel. The power of the heater after boiling is reduced to a minimum to avoid violent boiling.

All reagents (CuCl, $Na_2S$ * $9H_2O$) are put into a heated Teflon vessel at the same time.

After loading the charge, the vessel is filled with argon and tightly closed with a screw cap with a hole for steam release. During the course of the reaction, argon continues to flow into the upper part of the vessel, which creates some excess pressure over the surface of the melt.

The $Na_xCu_{1.75}S$ nanostructure is formed within several hours, usually held for 15 h at 165 °C. The formed crystals are in the melt in the form of a gel. The sizes of nanocrystallites can be varied by adding a small amount of water to the melt. The product obtained in the form of a gel clot is washed three times with heated distilled water, then washed with pure ethanol, and dried at room temperature.

From the powders, the tablets were prepared in the form of 2•5•20 $mm^3$ for measuring of the transport properties. Cold pressing under pressure of 2–3 tons/$cm^2$ was used. After pressing the annealing for 8 h at 450 °C in an argon atmosphere was provided for all samples.

X-ray phase analysis of the samples was carried out on a Bruker diffractometer (Germany) using radiation using $CuK_\alpha$ X-ray tube radiation and a graphite monochromator with a diffracted beam. The diffraction patterns were recorded in the range of 2θ angles from 20 to 65°, with a step of 2θ = 0.02°. The phases were identified using the BrukerAXSDIFFRAC.EVAv.4.2 software and the international database ICDD PDF-2.

The study of phase transitions and thermal effects in $Na_xCu_{2\text{-}x\text{-}y}S$ samples was carried out by differential scanning calorimetry method (DSC) with DSC 404 F1 Pegasus instrument (NETZSCH, Germany) in an argon atmosphere in the temperature range of 27–587 °C. The heating rate was 10 °C/min.

Mixed type of conductivity of the studied materials does not allow the use of conventional methods of conductivity measuring, so the electronic and the ionic conductivities were measured by well-known method of suppressing of undesirable current component, described, for example, in [22, 23]. To separate the electronic and ionic conductivity, one of the current components was suppressed by selecting the appropriate current electrodes and potential probes. For measurements of the ionic conductivity in the range of 330–440 °C, the Cu/CuBr current filters and potential probes were used. Ionic DC conductivities ($\sigma_i$) and chemical diffusion coefficients ($\tilde{D}$) were measured by a well-known Yokota's method [23] from curves of establishing and decay of concentration polarization. The applied electrochemical cell is shown in Fig. 1.

A constant ion current of 1 mA was passed through the $Na_xCu_{1.75}S$ sample using electrodes 1, 2 (Fig. 1) until a steady state was established. Steady potential difference $U_{ii}^{\infty}$ between ionic probes 3 and 4 was used to calculate the total ionic conductivity $\sigma_i = \sigma_{Na+} + \sigma_{Cu+}$ according to Ohm law

$$\sigma_i = \frac{Il}{(U_{ii}^{\infty} - U_{ii}^{o})S}, \tag{3}$$

where $I$ is the ionic current, $l$ is the distance between ionic probes 3 and 4, $S$ is a cross square of a sample, and $U_{ii}^{o}$ is the initial potential difference between ionic probes 3 and 4 before turning on the current. In our opinion, the measured ionic conductivity is a total cationic conductivity of the compound $\sigma_i = \sigma_{Na+} + \sigma_{Cu+}$.

After switching off the current, the time dependences of the potential difference $U_{ii}(t)$ between ion probes 3 and 4 were recorded. The chemical diffusion coefficient $\tilde{D}$ was calculated by the least squares method from the slope of the dependence $ln\ U_{ii}(t)$.

The measurements were performed in inert atmosphere of purified argon.

## X-ray phase analysis and differential scanning calorimetry

Figure 2 shows the powder X-ray diffraction patterns of the $Na_{0.15}Cu_{1.75}S$ (a), $Na_{0.20}Cu_{1.75}S$ (b), and $Na_{0.25}Cu_{1.75}S$ (c) samples taken at room temperature. Digits above pikes

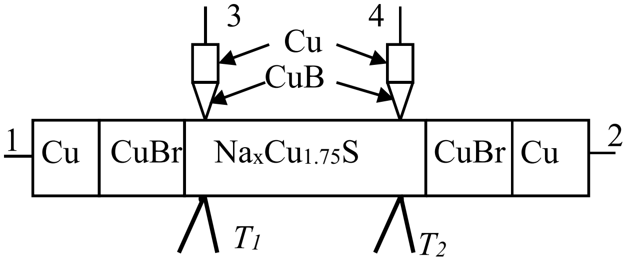

**Fig. 1** Scheme of the electrochemical cell for measurements of the ionic conductivity and chemical diffusion coefficient

denote as follows: 1 triclinic roxbyite, 2 orthorhombic anilite, 3 monoclinic $Na_2Cu_4S_3$, 4 cubic $Cu_2O$, 5 orthorhombic $Na_2S$.

Analysis of the spectra of Fig. 2 showed that samples of $Na_{0.15}Cu_{1.75}S$, $Na_{0.20}Cu_{1.75}S$, and $Na_{0.25}Cu_{1.75}S$ contain as the main phase the triclinic roxbyite $Cu_{1.8125}S$ with space group P $\overline{1}$ and cell parameters, $a = 13.4051$ (9), $b = 13.4090$ (8), $c = 15.4852$ (3) Å, $\alpha = 90.022$ (2), $\beta = 90.021$ (2), $\gamma = 90.020$ (3)° [24].

Roxbyite is a phase of variable composition with the formula $Cu_{1.74\div1.82}S$. The structure of roxbyite is based on a hexagonal-close-packed framework of sulfur atoms with the copper atoms occupying these layers, all having triangular coordination. The crystal structure of roxbyite bears a strong kinship to those of low chalcocite and djurleite. The authors of [25] draw attention to the propensity of roxbyite crystallites to twinning, which previously led to errors in determining the lattice symmetry and unit cell dimensions. However, twinning in nonstoichiometric copper sulfide leads to a decrease in the superionic transition temperature to a room temperature [25], and this is a positive point, since an increase in ionic conductivity at room temperature is very important for the commercialization of sodium-ion batteries.

Accordingly to Zh-H. Ge et al. [26], the solid solubility of Na in $Cu_{1.8}S$ did not exceed 3 at %. For $Na_{0.05}Cu_{1.8}S$ composition, the additional phases appear as $Na_2S$ and $Cu_{1.96}S$. Y.-X. Zhang et al. [27] noticed that a tiny amount of sodium sulfide hydrate ($Na_2S$ * $9H_2O$) doping into $Cu_{1.8}S$ can effectively suppress grain growth and create a porous structure during the fabrication procedure.

In our work along with the main phase, the studied samples contain impurities of orthorhombic anilite $Cu_{1.75}S$, sodium sulfide $Na_2S$, and cubic copper oxide $Cu_2O$. In all samples, the significant content of the monoclinic $Na_2Cu_4S_3$ phase, which is referred to as the so-called Scintl phases, was found.

The sizes of crystallites, estimated from the half-width of X-ray lines by the Williamson-Hall method, lie in the range from 13 to 82 nm in $Na_{0.15}Cu_{1.75}S$ alloy, from 10 to 113 nm in $Na_{0.20}Cu_{1.75}S$ alloy, and from 13 to 99 nm in $Na_{0.25}Cu_{1.75}S$ alloy which is due to approximately the same conditions for the synthesis in the melt of sodium and potassium hydroxides.

The $Na_2Cu_4S_3$ phase has a monoclinic lattice, space group C2/m (12). The number of atoms in a cell is 32. The lattice parameters are as follows: $a = 15.630$ Å, $b = 3.860$ Å, $c = 10.330$ Å, angle $\beta = 107.60°$. The density is low and equal to 4.173 g/cm$^3$. It is known that $Na_2Cu_4S_3$ crystallites have a chain structure and strong anisotropy [28]. At room temperature, for pressed samples, the conductivity of $Na_2Cu_4S_3$ is about 300 Om$^{-1}$ cm$^{-1}$. The ionic conductivity in $Na_2Cu_4S_3$ has not been studied, but the features of the crystal structure suggest a quasi-one-dimensional ionic conductivity in crystalline samples and a three-dimensional one in polycrystalline-pressed samples, however, lower than in $Cu_2S$.

Figure 3 shows, for example, a snapshot of the surface of the $Na_{0.25}Cu_{1.75}S$ sample. On Fig. 3a, the width of the field of view is 30 μm; piles of nanostrips up to 10-μm long and ~ 500- to 1000-nm wide are visible. In the lower left corner of Fig. 3a, an agglomerate of round or block particles with sizes up to 500 nm is observed. Figure 3b shows a surface Sect. 3.75-μm long in more detail, on which nanostrips and nanoplates of irregular shape are clearly visible. The particle sizes according to electron microscopy exceed by several times the estimated results from the X-ray line half-width. Perhaps this difference is due to the presence of sub-blocks inside the particles, due to which the estimate from the X-ray line half-width gives smaller sizes.

Figure 4 shows differential scanning calorimetry results for four compositions: $Cu_{1.75}S$, $Na_{0.15}Cu_{1.75}S$, $Na_{0.20}Cu_{1.75}S$, $Na_{0.25}Cu_{1.75}S$. The DSC curves demonstrate two strong thermal effects with critical temperatures of 116 ÷ 120 °C and 449 ÷ 453 °C.

For the $Cu_{1.75}S$ sample, the weak thermal effect is exhibited at 95 °C approximately, which can be correspond to phase transition from orthorhombic modification of anilite to hexagonal modification, but this phase transition usually takes place at 75 ± 3 °C [29]. The $Cu_{1.75}S$ sample was synthesized by the same method as the rest of the samples; according to X-ray studies, its composition is dominated by roxbyite with an admixture of anilite. According to W. G. Mumme et al. [30], a conversion of roxbyite to a digenite phase was observed to commence at 65–70 °C. Two modifications of digenite ($Cu_{1.8}S$) exists, a low-temperature trigonal form (below 91 °C) and high-temperature cubic Fm3m form (above 91 °C) [31, 32]. In our opinion, a wide (with a width of 40–50 °C) phase transition centered at 120 °C can be considered a structural transition to the superionic hexagonal phase of copper sulfide, the temperature of which depends on the stoichiometry of the composition [29]. $Na_2S$ and $Na_2Cu_4S_3$ did not undergo phase transition in the studied temperature interval.

The first thermal effect can be considered a transition to the hexagonal superionic phase, which is delayed by 13–16° relative to the transition point for coarse-grained copper sulfide, which can be attributed to the influence of impurities. The second thermal effect is close to the transition point from the hexagonal to the cubic form of pure copper sulfide (437 °C [33]), exceeding it also by 12–16°, which can also be attributed to the influence of impurity phases.

For the $Na_{0.15}Cu_{1.75}S$ composition, the peak of the thermal effect is located at 438 °C, practically coinciding with the critical temperature for pure coarse-grained copper sulfide. The same composition, as it turned out, has the activation energy

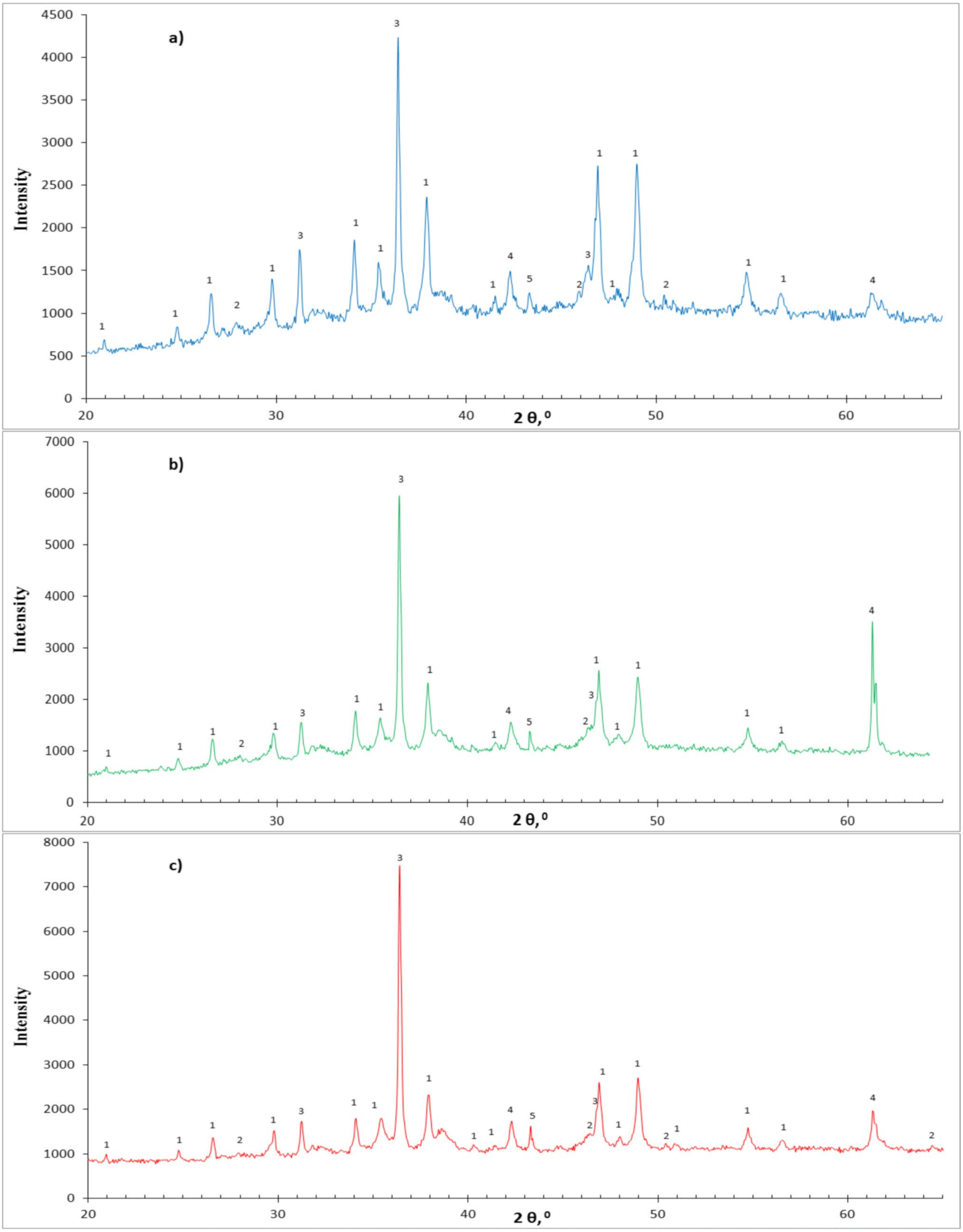

**Fig. 2** Powder diffraction patterns of the $Na_{0.15}Cu_{1.75}S$ (**a**), $Na_{0.20}Cu_{1.75}S$ (**b**), and $Na_{0.05}Cu_{1.75}S$ (**c**) samples taken at room temperature. Digits above pikes denote 1 triclinic roxbyite, 2 orthorhombic anilite, 3 monoclinic $Na_2Cu_4S_3$, 4 cubic $Cu_2O$, and 5 orthorhombic $Na_2S$ phases

**Fig. 3** Image of the $Na_{0.25}Cu_{1.75}S$ powder taken with MIRA3 TESCAN scanning electron microscope. Piles of nanostrips up to 10-μm long and ~ 500- to 1000-nm wide are visible (**a**); in the lower left corner of Fig. 3a, an agglomerate of round or block particles with sizes up to 500 nm is observed. Figure 3b shows a surface Sect. 3.75-μm long in more detail, on which nanostrips and nanoplates of irregular shape are clearly visible

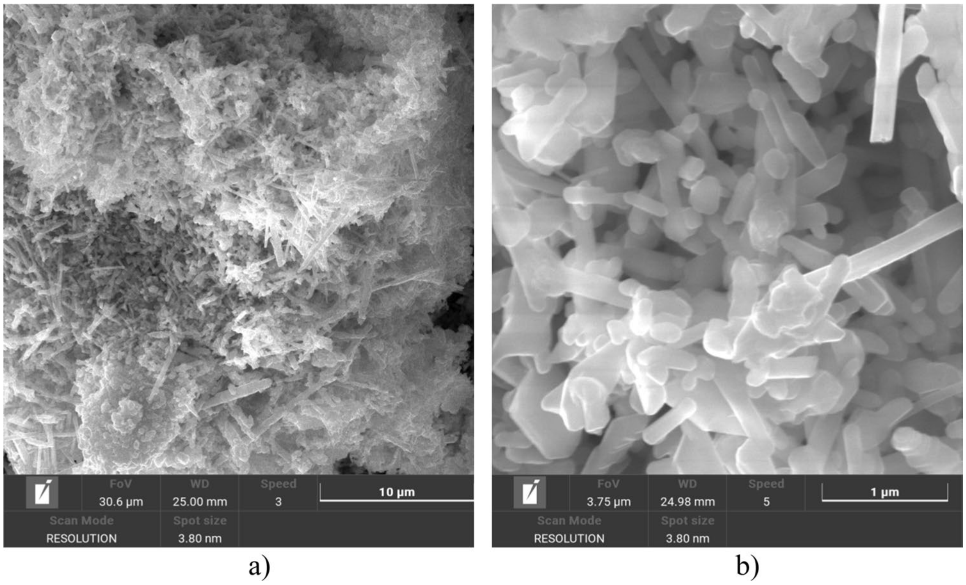

a) b)

**Fig. 4** Curves of differential scanning calorimetry of $Cu_{1.75}S$, $Na_{0.15}Cu_{1.75}S$, $Na_{0.20}Cu_{1.75}S$, and $Na_{0.25}Cu_{1.75}S$ samples recorded in argon atmosphere

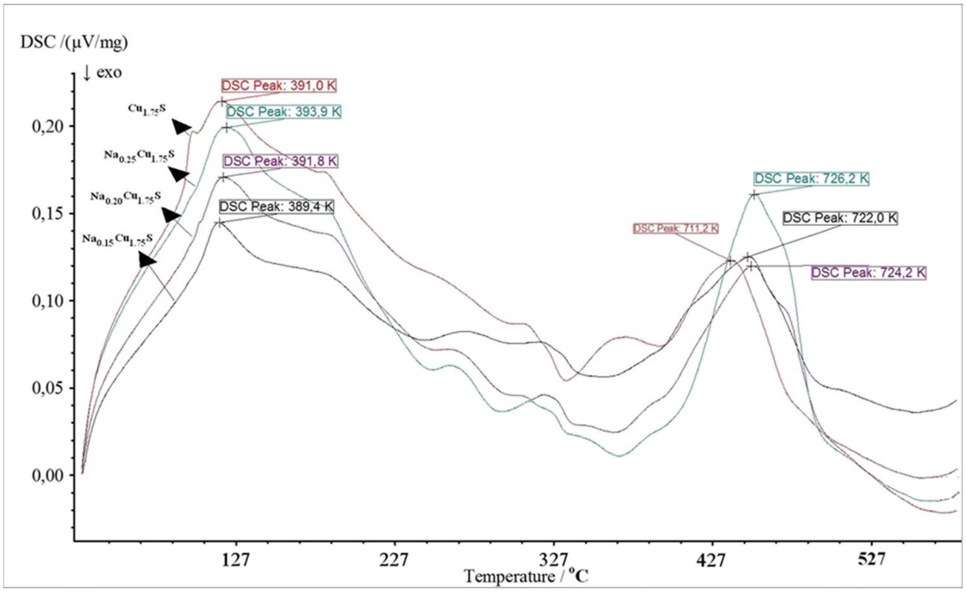

of ionic conductivity much lower than that of other samples (Table 1).

## Ionic conductivity and chemical diffusion

The curves of establishing and decay of the concentration polarization were taken for all three samples at temperatures 370, 380, 390, 400, and 410 °C with using the electrochemical cell, presented in Fig. 1. For example, one such curve is shown in Fig. 5a for $Na_{0.15}Cu_{1.75}S$ sample at 370 °C.

Ionic conductivities were calculated accordingly to Eq. (2) using ($U_{ii}^{\infty} - U_{ii}^{o}$) difference determined from taken concentration polarization curves. The temperature

**Table 1** Parameters of the ionic transport of the $Na_xCu_{1.75}S$ materials

| Sample | Activation energy of the ionic conductivity, eV | Activation energy of the chemical diffusion, eV |
|---|---|---|
| $Na_{0.10}Cu_{1.75}S$ | 1.10 ± 0.05 (below 390 °C)<br>0.30 ± 0.02 (above 390 °C) | 1.87 ± 0.09 |
| $Na_{0.15}Cu_{1.75}S$ | 0.40 ± 0.02 | 0.36 ± 0.02 |
| $Na_{0.20}Cu_{1.75}S$ | 1.03 ± 0.05 | 2.57 ± 0.15 |

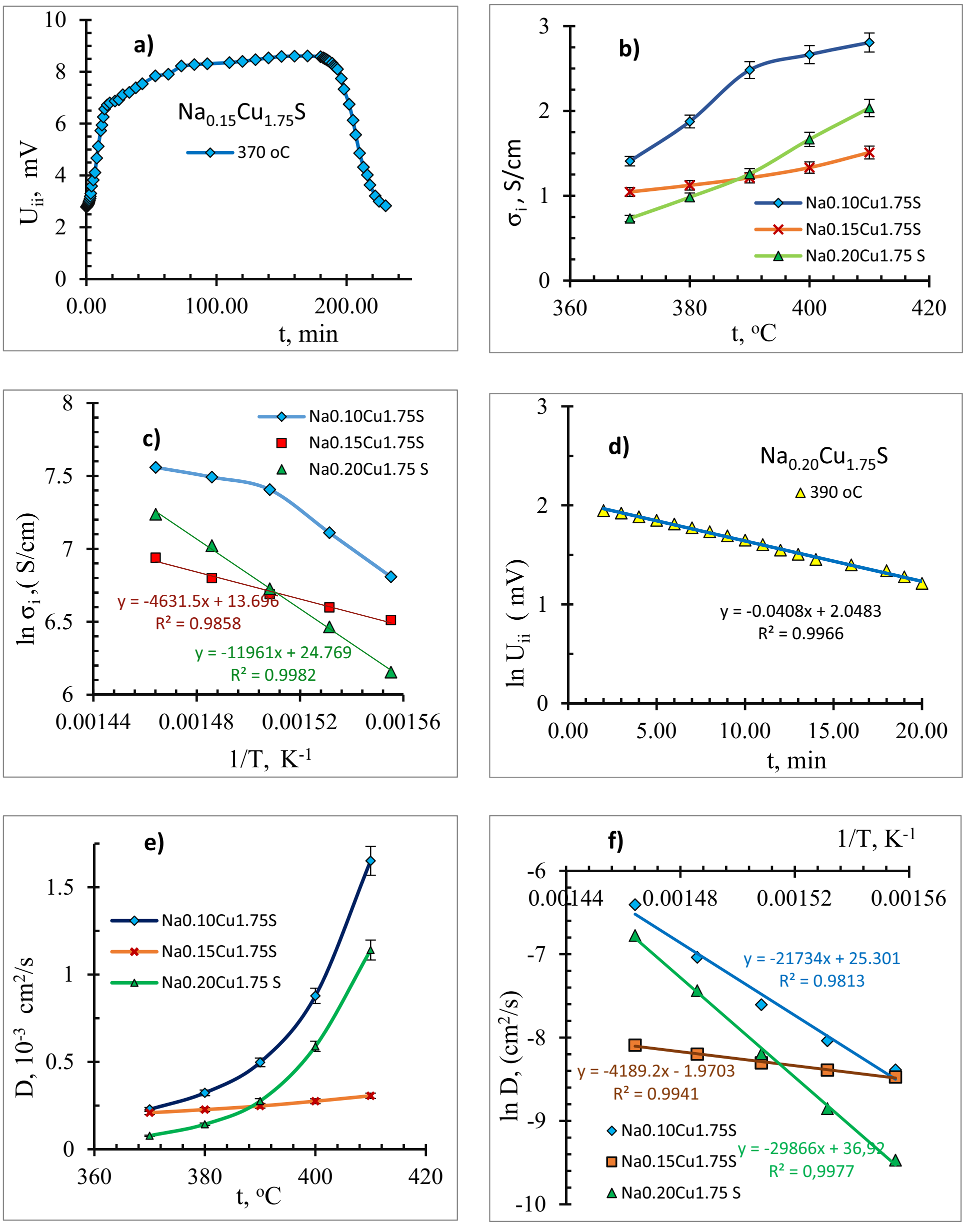

**Fig. 5** **a** The curve of establishing and decay of the concentration polarization at switching on and off the direct ionic current 1 mA through the Cu/CuBr/$Na_{0.15}Cu_{1.75}S$/CuBr/Cu electrochemical cell at 370 °C; **b** temperature dependences of the ionic conductivity for $Na_{0.10}Cu_{1.75}S$, $Na_{0.15}Cu_{1.75}S$, and $Na_{0.20}Cu_{1.75}S$ samples; **c** temperature dependences of the ionic conductivity for $Na_{0.10}Cu_{1.75}S$, $Na_{0.15}Cu_{1.75}S$, and $Na_{0.20}Cu_{1.75}S$ samples in ln $\sigma_i$T—(1/T) coordinates; **d** time dependences of the decay of the concentration polarization plotted in semilogarithmic coordinates for the $Na_{0.20}Cu_{1.75}S$ sample; **e** temperature dependences of the conjugated chemical diffusion coefficient of cations and electron holes for $Na_{0.10}Cu_{1.75}S$, $Na_{0.15}Cu_{1.75}S$, and $Na_{0.20}Cu_{1.75}S$ samples; **f** temperature dependences of the chemical diffusion coefficient of $Na_{0.15}Cu_{1.75}S$ plotted in ln D—(1/T) coordinates

dependences of the ionic conductivities are presented in Fig. 5b. As it seen in Fig. 5b, the ionic conductivity decreases with Na content in the compounds, but values of the ionic conductivity remain high (> 0.6 S/cm at 370 °C).

To determine the activation energy of the ionic conductivity, auxiliary graphs ln $\sigma_i$ T (1/T) were plotted as shown in Fig. 5c.

All lines in Fig. 5c demonstrate linear character accordingly in Arrhenius law. Calculated from the slope of the obtained straight lines, the activation energy values are presented in the Table 1. The temperature dependence of the ionic conductivity of $Na_{0.15}Cu_{1.75}S$ in Fig. 5c shows a kink at 390 °C, in which there is an abrupt change in the activation energy without a jump in ionic conductivity. Below this temperature, the activation energy is 0.30 eV; above this temperature, it becomes 1.10 eV. As follows from the DSC calorimetry data (Fig. 4), a prolonged phase transition begins at 370 °C in the materials under study, which finally ends above 500 °C. It is somewhat incorrect to measure the activation energy of conduction in the region of the phase transition, so we will refrain from drawing any definite conclusions from these data.

To calculate the coefficient of conjugated diffusion of cations and electronic holes from the concentration polarization decay curves, the graphs of the logarithm of the $U_{ii}(t)$ dependence were plotted, similar to one shown in Fig. 5d for the $Na_{0.20}Cu_{1.75}S$ sample. It can be seen that the experimental points in the coordinates *ln* $U_{ii} = f(t)$ fit well on a straight line, which makes it possible to accurately determine the coefficient of conjugate diffusion of copper cations and electron holes $\tilde{D}$ in accordance with expression (1). The measurement error $\tilde{D}$ was no more than 4–5%.

Received temperature dependences of the coefficient $\tilde{D}$ of conjugate chemical diffusion for $Na_xCu_{1.75}S$ samples obtained at 370–410 °C are shown in Fig. 5e. The chemical diffusion coefficient has the highest values for solids, reaching $1.6•10^{-3}$ $cm^2s^{-1}$. As can be seen from these figures, the temperature dependences for all compositions have an Arrhenius character.

To determine the activation energy of chemical diffusion, auxiliary graphs ln D (1/T) were plotted as shown in Fig. 5f. Calculated from the slope of the straight lines in Fig. 5f, the values of the activation energy of chemical diffusion are shown in Table 1.

In coarse-grained copper sulfide $Cu_{1.98}S$, the transition from the hexagonal to the cubic modification occurs at about 367 °C, also without a jump in ionic conductivity, and the activation energy of ionic conductivity decreases from 0.47 to 0.29 eV [34]. For nanosized $Na_{0.15}Cu_{1.75}S$, the activation energy of the ionic conductivity is close to one for coarse-grained copper sulfide. For the $Na_{0.10}Cu_{1.75}S$ and $Na_{0.20}Cu_{1.75}S$ compositions, the activation energies are three times higher than those for coarse-grained copper sulfide. It is possible that the distribution of cations over the interstices of the superionic conductor changes, and deeper potential wells appear which increase the activation energy. Other reasons may be both the incompleteness of the phase transition in the measurement interval and the influence of interphase boundaries, since the material is not homogeneous, and there is an admixture of a non-superionic phase ($Cu_2O$).

As can be seen from Table 1, with an increase in the sodium content in the material, the chemical diffusion coefficient decreases slightly, but it remains very high. The activation energy of chemical diffusion is minimal for $Na_{0.15}Cu_{1.75}S$ composition, which corresponds to the idea of mixing two salts with conductivity for different alkali metal ions (mixed-alkali effect).

## Conclusion

The process of conjugate chemical diffusion of ions and electrons (holes) in copper chalcogenides proceeds under the influence of a gradient of the degree of nonstoichiometry. Due to the action of the principle of electroneutrality, diffusion jumps of ions in a mixed electron–ion conductor lead to the same movement of matter as the jumps of neutral atoms. The resulting internal electric field accelerates the movement of “slow” particles (cations) and accelerates the movement of “fast” particles (electron holes) [10]. This explains the observed high values of CCDC in the studied electron–ion conductors $Na_{0.10}Cu_{1.75}S$, $Na_{0.15}Cu_{1.75}S$, and $Na_{0.20}Cu_{1.75}S$. The chemical diffusion coefficient of the compositions has the highest values for solids, reaching $1.6•10^{-3}$ $cm^2s^{-1}$ for $Na_{0.10}Cu_{1.75}S$ alloy at 410 °C. Nevertheless presence of sodium in the lattice essentially changes the conditions of the ionic transport in comparison with binary copper sulfide. For the $Na_{0.10}Cu_{1.75}S$ and $Na_{0.20}Cu_{1.75}S$ compositions, the activation energies of the ionic conductivity are three times higher than those for coarse-grained copper sulfide. The activation energies of the conjugate chemical diffusion for these compositions are roughly two times higher than those for their ionic conductivities.

The high values of the chemical diffusion coefficients in sodium-substituted copper sulfides allow us to hope for an increase in the operating current density of sodium-ion batteries using copper sulfides as an active electrode material.

**Funding** This research was funded by the Science Committee of the Ministry of Education and Science of the Republic of Kazakhstan (no. AP08856636).

## References

1. Hwang J-Y, Myung S-T, Sun Y-K (2017) Sodium-ion batteries: present and future. Chem Soc Rev 45:3529–3614. https://doi.org/10.1039/c6cs00776g
2. Ohno S, Banik A, Dewald GF, Kraft MA, Krauskopf T, Minafra N, Till P, Weiss M, Zeier WG (2020) Materials design of ionic conductors for solid state batteries. Progress Energy 2(2):022001. https://doi.org/10.1088/2516-1083/ab73dd
3. Hu Z, Liu Q, Lai W, Gu Q, Li L, Chen M, Wang W, Chou S, Liu Y, Dou S (2020) Manipulating molecular structure and morphology to invoke high-performance sodium storage of copper phosphide. Adv Energy Mater 10(19):1903542. https://doi.org/10.1002/aenm.201903542
4. Han L, Wu S, Hu Z, Chen M, Ding J, Wang S, Zhang Y, Guo D, Zhang L, Cao S, Chou S (2020) Hierarchically porous $MoS_2$–carbon hollow rhomboids for superior performance of the anode of sodium-ion batteries. ACS Appl Mater Interfaces 12(9):10402–10409. https://doi.org/10.1021/acsami.9b21365
5. Kim J-S, Kim D-Y, Cho G-B, Nam T-H, Kim K-W, Ryu H-S, Ahn J-H, Ahn H-J (2009) The electrochemical properties of copper sulfide as cathode material for rechargeable sodium cell at room temperature. J Power Sources 189(1):864–868. https://doi.org/10.1016/j.jpowsour.2008.10.057
6. Yue J-L, Sun Q, Fu Z-W (2013) Cu2Se with facile synthesis as a cathode material for rechargeable sodium batteries. Chem Commun 49(52):5868. https://doi.org/10.1039/c3cc41934g
7. Kubenova MM, Kuterbekov KA, Balapanov MK, Ishembetov RK, Kabyshev AM, Bekmyrza KZ (2021) Some thermoelectric phenomena in copper chalcogenides replaced by lithium and sodium alkaline metals. Nanomaterials 11(9):2238. https://doi.org/10.3390/nano11092238
8. Balapanov MKh, Kubenova MM, Kuterbekov KA, Kozlovskiy A, Nurakov SN, Ishembetov RKh, Yakshibaev RA (2018) Phase analysis, thermal and thermoelectric properties of nanocrystalline

$Na_{0.15}Cu_{1.85}S$, $Na_{0.17}Cu_{1.80}S$, $Na_{0.20}Cu_{1.77}S$ alloys. Eurasian J Phys Funct Mater 2(3):231–241. https://doi.org/10.29317/ejpfm.2018020304

9. Balapanov MKh, Ishembetov RKh, Kuterbekov KA, Kubenova MM, Almukhametov RF, Yakshibaev RA (2017) Transport phenomena in superionic $Na_xCu_{2-x}S$ (x = 0.05; 0.1; 0.15; 0.2) compounds. Ionics 24(5): 1349–1356. https://doi.org/10.1007/s11581-017-2299-z
10. Chebotin VN (1989) Chemical diffusion in solids. Nauka, Moscow, p 208
11. Miyatani S (1973) Electronic and ionic conduction in $(Ag_xCu_{1-x})_2Se$. J Phys Soc Japan 34(2):423–432. https://doi.org/10.1143/jpsj.34.423
12. Rickert H, Wiemhofer HD (1983) Measurements of chemical diffusion coefficients of mixed conducting solids using point electrodes-investigations on $Cu_2S$. Solid States Ionics 11:257. https://doi.org/10.1016/0167-2738(83)90032-2
13. Rickert H, Wiemhofer HD (1983) Stability behaviour of mixed conducting solids after applying electrical potential differences — measurements with point electrodes on $Ag_2S$ and $Cu_2S$. Ber Bunsenges Phys Chem 87:236. https://doi.org/10.1002/bbpc.19830870313
14. Tinter U, Wiemhofer HD (1983) Chemical diffusion coefficients of the low temperature phases of CuxSe and $Cu_xS$ - investigations with point electrodes. Solid State Ionics 9–10:1213. https://doi.org/10.1016/0167-2738(83)90154-6
15. Cassaignon S, Pauport Th, Guillemoles J-F, Vedel J (1998) Copper diffusion in copper sulfide: a systematic study. Ionics 4:364–371. https://doi.org/10.1007/BF02375879
16. Balapanov MKh, Urazaeva EK, Zinnurov IB, Musalimov RSh, Yakshibaev RA (2006) Influence of grain sizes on the ionic conductivity and the chemical diffusion coefficient in copper selenide. Ionics 12:205–209. https://doi.org/10.1007/s11581-006-0027-1
17. Chebotin VN, Konev VN, Berezin VM (1984) Himicheskaja diffuzija v nestehiometricheskih tverdyh rastvorah $(Cu_{1-x}Ag_{x+\delta})$2X, gde H-S. Se Izvestija AN SSSR Neorganicheskie Mater 20(9):1462–1466 (in Russian)
18. Balapanov MKh, Yakshibaev RA, Mukhamed'yanov UKh (2003) Ion transfer in solid solutions of $Cu_2Se$ and $Ag_2Se$ superionic conductors. Phys Solid State 45(4):634–638. https://doi.org/10.1134/1.1568997
19. Balapanov MKh, Nadejzdina AF, Yakshibayev RA, Lukmanov DR (1999) Ionic conductivity and chemical diffusion in $Li_xCu_{2-x}Se$ superionic alloys. Ionics 5:20–22. https://doi.org/10.1007/BF02375898
20. Balapanov MKh, Bickulova NN, Mukhamedyanov UKh, Asilguschina GN, Musalimov RSh, Zeleev MKh (2004) Phase transitions and transport phenomena in $Li_{0.25}Cu_{1.75}Se$ superionic compound. Phys Stat Sol (b) 241(15):3517–3524. https://doi.org/10.1002/pssb.200402076
21. Balapanov MKh, Gafurov IG, Mukhamed'yanov UKh, Yakshibaev RA, Ishembetov RKh (2004) Ionic conductivity and chemical diffusion in superionic $Li_xCu_{2-x}S$ ($0 < x < 0.25$). Phys Stat Sol (b) 241(1):114–119. https://doi.org/10.1002/pssb.200301911
22. Weppner W, Huggins RA (1978) Electrochemical methods for determining kinetic properties of solids. Ann Rev Mater Sci 8:269–311. https://doi.org/10.1146/annurev.ms.08.080178.001413
23. Yokota I (1961) On the theory of mixed conduction with special reference to conduction in silver sulfide group semiconductors. J Phys Soc Jpn 16:2213–2223. https://doi.org/10.1143/JPSJ.16.2213
24. Mumme WG, Gable RW, Petricek V (2012) The crystal structure of roxbyite, $Cu_{58}S_{32}$. Can Mineral 50:423. https://doi.org/10.3749/canmin.50.2.423
25. Gong J, Jain PK (2019) Room-temperature superionic-phase nanocrystals synthesized with a twinned lattice. Nat Commun 10:3285. https://doi.org/10.1038/s41467-019-11229-2
26. Ge Z-H, Liu X, Feng D, Lin J, He J (2016) High-performance thermoelectricity in nanostructured earth-abundant copper sulfides bulk materials. Advanced Energy Mat 6(16):1600607. https://doi.org/10.1002/aenm.201600607
27. Zhang Y-X, Feng J, Ge Zh-H (2020) High thermoelectric performance realized in porous $Cu_{1.8}S$ based composites by $Na_2S$ addition. Mater Sci Semiconduct Process 107:104848. https://doi.org/10.1016/j.mssp.2019.104848
28. Schafer SH (1981) Zur kenntnis von $Na_2Cu_4S_3$ und $KCu_3Te_2$. Mater Res Bull 16(10):1291–1297. https://doi.org/10.1016/0025-5408(81)90100-8
29. Chakrabarti DJ, Laughlin DE (1983) The Cu-S (Copper-Sulfur) system. J Phase Equilibria 4(3):254–271. https://doi.org/10.1007/bf02868665
30. Mumme WG, Sparrow GJ, Walker GS (1988) Roxbyite, a new copper sulphide mineral from the Olympic Dam deposit, Roxby Downs, South Australia. Mineral Mag 52:323–330. https://doi.org/10.1180/minmag.1988.052.366.03
31. Will G, Hinze E, Abdelrahman AR (2002) Crystal structure analysis and refinement of digenite, $Cu_{1.8}S$, in the temperature range 20 to 500 °C under controlled sulfur partial pressure. Eur J Miner 14:591–598. https://doi.org/10.1127/0935-1221/2002/0014-0591
32. Kashida S, Yamamoto K (1991) An X-ray study of the incommensurate structure in digenite ($Cu_{1.8}S$). J Phys Condens Matter 3:6559. https://doi.org/10.1088/0953-8984/3/34/001
33. Gronvold F, Westrum EF (1987) Thermodynamics of copper sulfides I. Heat capacity and thermodynamic properties of copper (I) sulfide, $Cu_2S$, from 5 to 950 K. J Chem Thermodyn 19:1183–1198. https://doi.org/10.1016/0021-9614(87)90056-5
34. Balapanov MKh, Zinnurov IB, Mukhamed'yanov UKh, Musalimov RSh (2007) Ionic conduction and chemical diffusion in $Cu_{2-x}S$ codoped with magnesium and aluminum. Inorg Mater 43(5):449–451. https://doi.org/10.1134/s0020168507050019